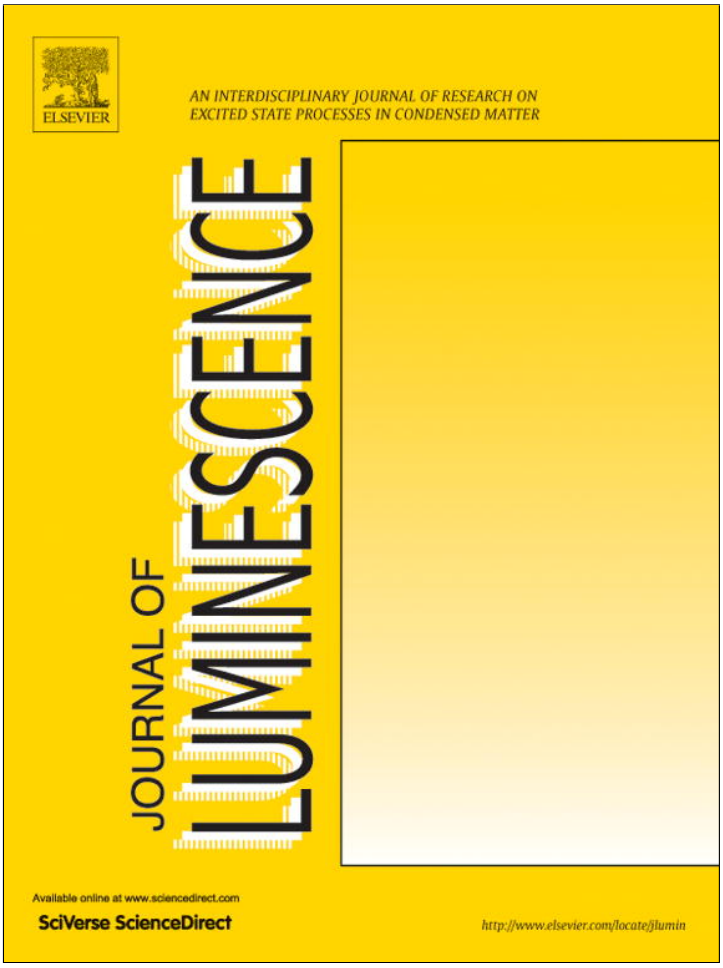
ELSEVIER
AN INTERDISCIPLINARY JOURNAL OF RESEARCH ON EXCITED STATE PROCESSES IN CONDENSED MATTER
JOURNAL OF
LUMINESCENCE
Available online at www.sciencedirect.com
SciVerse ScienceDirect
http://www.elsevier.com/locate/jlumin

Journal of Luminescence 141 (2013) 106–110

Contents lists available at SciVerse ScienceDirect

Journal of Luminescence

journal homepage: www.elsevier.com/locate/jlumin

# Enhanced luminance for inorganic electroluminescent devices with a charged electret

Fang-Hsing Wang [a,*], Kuo-Feng Chen [a,b], Yu-Han Chien [b], Chin-Chia Chang [b], Meng-Ying Chuang [b]

[a] Department of Electrical Engineering and Graduate Institute of Optoelectronic Engineering, National Chung Hsing University, Taichung 402, Taiwan, ROC
[b] Display Technology Center/Industrial Technology Research Institute, Hsinchu 310, Taiwan, ROC

ARTICLE INFO

*Article history:*
Received 25 September 2012
Received in revised form
11 March 2013
Accepted 15 March 2013
Available online 25 March 2013

*Keywords:*
Electroluminescent (EL)
Inorganic
Powder
Electret

ABSTRACT

This work proposes a novel inorganic electroluminescent (IEL) device with an electric field built-in (EFBI) technique to reduce its driving voltage and enhance its luminance. The EFBI technique was performed by charging an electret comprising a silicon dioxide film at different temperatures (25–150 °C) in powder electroluminescent (PDEL) devices. The driving voltage of the EFBI-PDEL device decreased by 61.4 V (or 20.5%) under the brightness of 269 cd/m$^2$, and its brightness increased by 128 cd/m$^2$ (or 47%) at ac 300 V. The efficiency of the EFBI-PDEL device significantly increased by 0.827 lm/W (or 45.5%) at ac 300 V. The proposed EFBI-PDEL device has advantages of a low-temperature process and low cost, and potential for large-area display applications.



## 1. Introduction

Powder EL devices (PDELs) possess many advantages including wide viewing angles, wide operating temperature ranges, and inherent ruggedness [1–3]. PDEL devices are easily manufactured using a printing process, which possesses advantages including low-temperature processes, large-area producibilities, and low cost. PDEL is currently one of many potential technologies in the field of information display, and has many valuable applications in backlight units, displays, and billboards. However, the high driving voltage limits the development of PDEL devices in commercial applications. Many studies have been proposed to improve the performance of PDEL devices [4–6]. Kim et al. fabricated an alternating current inorganic PDEL device with a top-emission structure [4]. Its efficiency and brightness increased by 50% and 40%, respectively, compared with that with the bottom-emission structure. In our previous research, a carbon nanotube (CNT)-incorporated dielectric layer was introduced into PDEL devices to reduce power consumption and enhance luminous efficiency [6]. An increase of 50% in luminous efficiency was achieved after single-walled CNTs were added into the devices. This study introduces a charged electret into a PDEL device to enhance its device performance. The electret is composed of materials that can be electrically charged [7–12]. By using a thermal charging process, electrical charges can be injected into the electret and trapped in defect sites. The effects of the charging temperature and time on brightness and efficiency of the PDEL device are investigated.

## 2. Experimental methods

The fabrication process of the proposed PDEL device, called the electric field built-in (EFBI)–PDEL device, is divided into three parts: the top substrate process, the bottom substrate process, and the EFBI process. The top and bottom substrates were combined and sealed to form the EFBI-PDEL device. The detailed fabrication processes are as follows:

This experiment used flexible transparent substrates (polyethylene terephthalate, PET) as the top and bottom substrates. An indium-tin-oxide (ITO) film with a thickness of approximately 180 nm was first sputtered on the top substrate. A ZnS-based phosphor (DuPont LuxPrint 8150L paste) was then coated by using screen printing, and then baked at 130 °C for 10 min. The thickness of the phosphor layer was approximately 40 μm. Finally, a dielectric layer ($BaTiO_3$, DuPont LuxPrint 8153 paste) was coated on the phosphor layer by using screen printing, and then baked at 130 °C for 5 min. The thickness of the dielectric layer was approximately 14 μm. Fig. 1(a) and (b) shows the cross-section and plane-view SEM photographs of dielectric/phosphor layers. The particle sizes of the phosphor and dielectric layer are approximate 15 ± 3 and 0.6 ± 0.2 μm. In the bottom substrate process, an ITO film was deposited by radio frequency (RF) sputtering. Thereafter, silicon nitride ($SiN_x$) and silicon oxide ($SiO_x$) thin films were deposited

* Corresponding author. Tel.: +886 4 22840688x706; fax: +886 4 22851410.
*E-mail address:* fansen@dragon.nchu.edu.tw (F.-H. Wang).

0022-2313/$ - see front matter © 2013 Elsevier B.V. All rights reserved.
http://dx.doi.org/10.1016/j.jlumin.2013.03.020

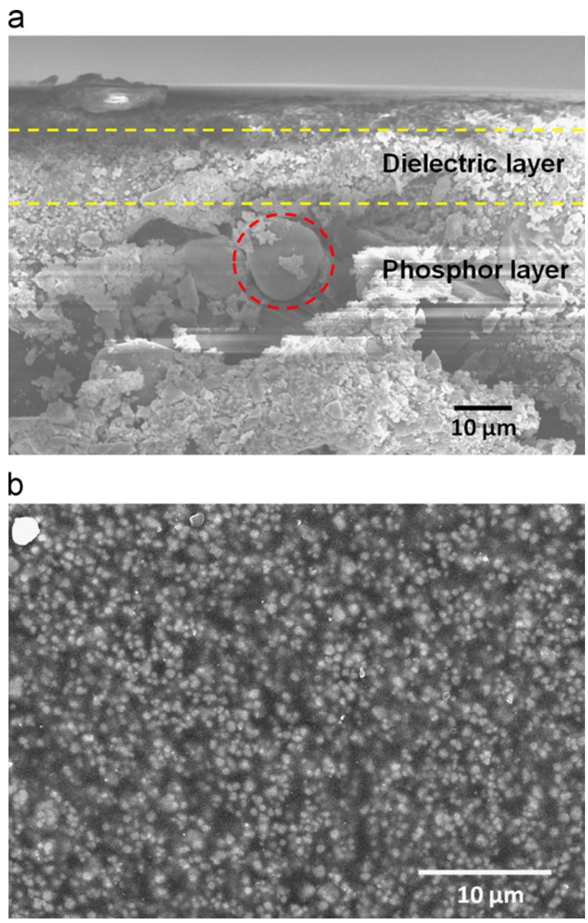


**Fig. 1.** (a) cross-section and (b) plane-view SEM photographs of dielectric/phosphor layers.

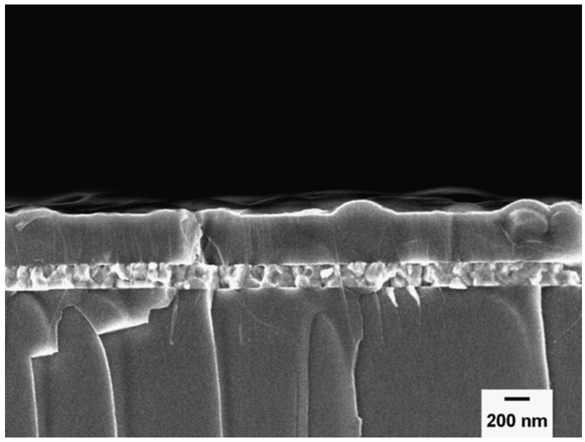


**Fig. 2.** The cross-section SEM photograph of the $SiO_x/SiN_x$/ITO thin films.

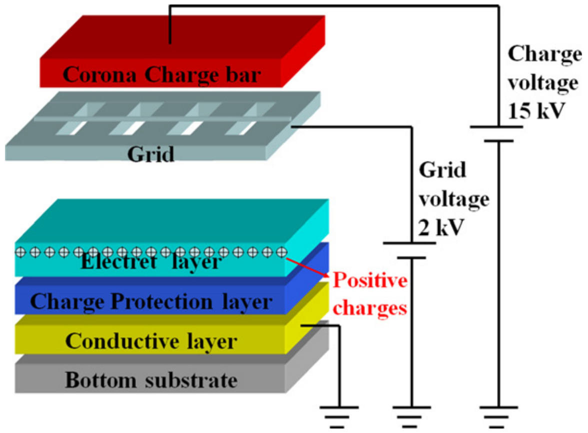


**Fig. 3.** Schematic diagram of the corona charging system used in this study.

continuously by using plasma-enhanced chemical vapor deposition (PECVD) as a charge protection and an electret layers, respectively. The deposition temperature was 130 °C, and the RF powers were 340 W and 300 W for the $SiN_x$ and $SiO_x$ films, respectively. Fig. 2 exhibits the cross-section SEM photograph of the $SiO_x/SiN_x$/ITO thin films. The thickness of the $SiO_x/SiN_x$/ITO thin films are approximate 160/250/180 nm. The equivalent dielectric constant of $SiN_x+SiO_x$ film measured from the capacitance-voltage characteristics was 4.9. The area of the devices is 4.25 cm × 4.25 cm. This experiment uses a corona charging system to charge the electret, as shown in Fig. 3. The charging process was divided into three steps: (1) pre-annealing at 50 °C for 10 min, (2) thermal charging at a temperature of 25–150 °C for 5–30 min, and (3) post-annealing at 50 °C for 10 min. Heating in the charging process could increase the opportunity of charge trapping in deep-level defects, and hence, enhance the accumulated charges in the electret [13]. The charging ambient air was at a pressure of approximately 760 Torr. The distance between the grid and the $SiO_x$ layer was 10 cm, and the space between the corona bar and the grid was 5 cm. The voltages of the charging bar and the grid were 15 kV and 2 kV, respectively. After charging, the top and the bottom substrates were bonded together using a lamination machine to complete the device process. The luminance was measured by a luminance colorimeter (KLEIN, K8).

## 3. Results and discussion

The structures and equivalent circuit models of the traditional PDEL device and the proposed EFBI-PDEL device are shown in

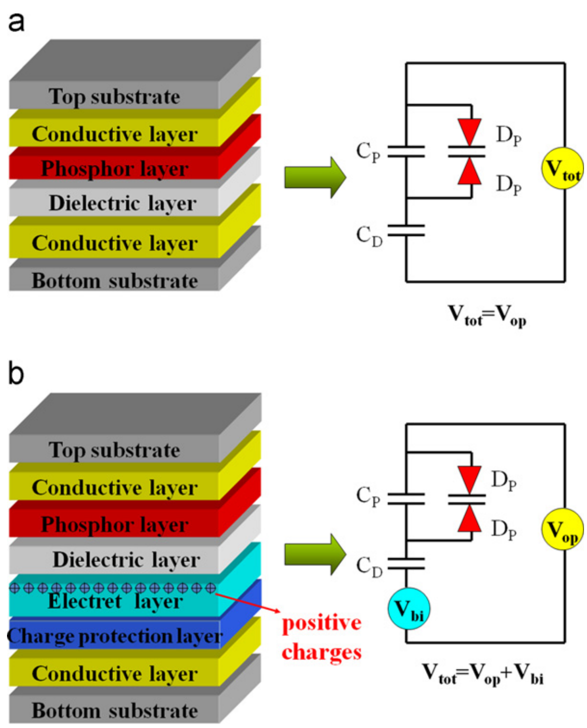


**Fig. 4.** Schematic structures and device circuit model of the traditional PDEL device and the proposed EFBI-PDEL device.

Fig. 4. The phosphor layer is defined as a capacitor ($C_P$) parallel to a zener diode ($D_P$). The dielectric layer is defined as capacitor ($C_D$). The electret can be charged to produce a built-in electric field, and is defined as an equivalent voltage $V_{bi}$. According to Kirchhoff's circuit laws, the external voltage ($V_{op}$) and the build-in voltage ($V_{bi}$) are in series connection with each other. Therefore, the driving voltage of the charged EFBI-PDEL device is defined as $V_{tot}=V_{op}+V_{bi}$. By adding extra $V_{bi}$ in the PDEL device, the external driving voltage can be reduced.

This study used simulation software (Silvaco, ATLAS) to locate the built-in electric field in the PDEL devices. The charge densities were assumed at $5.7\times10^{-7}$, $6.7\times10^{-7}$, $9.6\times10^{-7}$, and $1.5\times10^{-6}$ C/cm$^2$. The built-in potential can be calculated from the built-in charge density using the following equation [14]:

$$V=\frac{Q}{\varepsilon_1\times\varepsilon_0/d_1+\varepsilon_2\times\varepsilon_0/d_2} \tag{1}$$

where $\varepsilon_1$, $\varepsilon_2$ are the dielectric constants, $\varepsilon_0$ is the permittivity of the vacuum, and $d_1$, $d_2$ are the thicknesses of the silicon oxide and silicon nitride films, respectively. In this study, $\varepsilon_1$, $\varepsilon_2$, $d_1$, and $d_2$ are 3.8, 7.5, 300 nm, and 500 nm, respectively. The calculated built-in electric fields at the interface between the dielectric layer and the electret were $1.38\times10^5$, $1.64\times10^5$, $2.41\times10^5$, and $3.74\times10^5$ V/cm, and the calculated $V_{bi}$ were 23.2, 27.3, 39.2, and 61.4 V for the charge densities of $5.7\times10^{-7}$, $6.7\times10^{-7}$, $9.6\times10^{-7}$ and $1.5\times10^{-6}$ C/cm$^2$, respectively. The simulation results show that the built-in electric field existing inside the EFBI-PDEL device depends on the built-in electric charge density on the electret.

Fig. 5 shows the brightness of the EFBI-PDEL devices charged at different temperatures as a function of driving voltages (rms). The charging temperature is 25 °C, 50 °C, 100 °C, and 150 °C for 30 min. The brightness and driving voltage of the devices is shown in Table 1. Results showed that with the rise of charging temperature from 25 to 150 °C, the brightness increased from 13% to 47% compared with the uncharged device. At a fixed brightness of 269 cd/m$^2$, the driving voltage decreased from 7.7% to 20.5%, as shown in Table 1. The optimal charging temperature is 150 °C in this study. A further increase in charging temperature is prohibited because of the limitations of the equipment. The enhanced device performance is due to the charges in the electret possessing more energy at higher temperatures and being able to be trapped at deeper levels, which produces more stable trapped charges and higher charge densities, thus causing a larger built-in electric field in the devices [13,15].

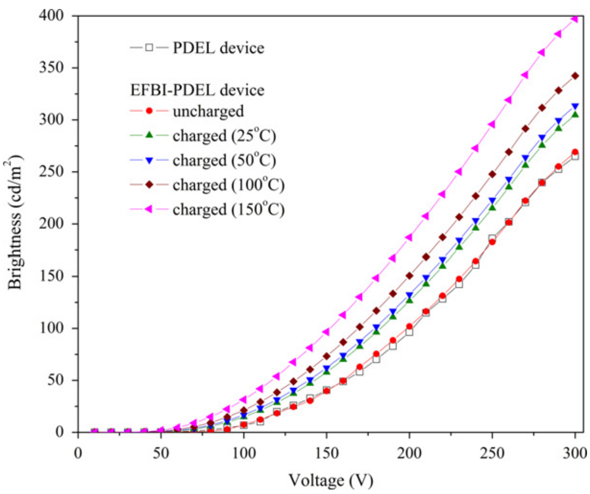


**Fig. 5.** Brightness of the EFBI-PDEL devices charged at different temperatures as a function of driving voltage (rms).

**Table 1**
Brightness and driving voltages of the PDEL devices with difference charging temperatures.

| | Uncharged device | Charged devices | | | |
|---|---|---|---|---|---|
| Charging temperature (°C) @ 30 min | – | 25 | 50 | 100 | 150 |
| Brightness (cd/m$^2$) @ 300 V | 269 | 304 | 313 | 342 | 397 |
| Driving voltage (V) @ 269 cd/m$^2$ | 300 | 276.8 | 272.2 | 260.8 | 238.6 |

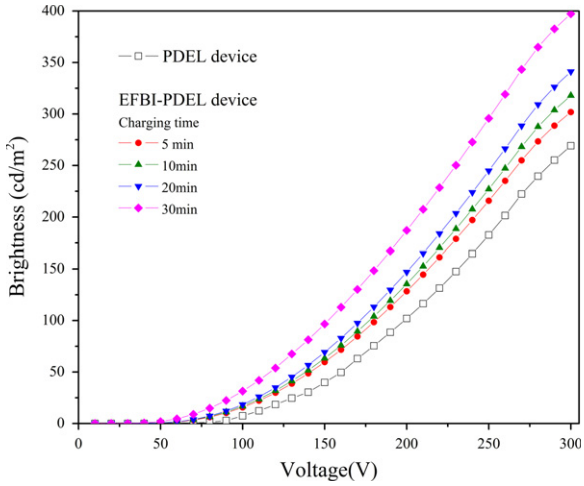


**Fig. 6.** Brightness of the EFBI-PDEL devices with different charging times as a function of driving voltage (rms).

**Table 2**
Brightness and driving voltages of the PDEL devices with difference charging times.

| | Uncharged device | Charged devices | | | |
|---|---|---|---|---|---|
| Charging time (min) @ 150 °C | – | 5 | 10 | 20 | 30 |
| Brightness (cd/m$^2$) @ 300 V | 269 | 301 | 318 | 341 | 397 |
| Driving voltage (V) @ 269 cd/m$^2$ | 300 | 277.2 | 268.2 | 258.0 | 238.6 |

The brightness of the EFBI-PDEL devices with different charging times as a function of driving voltage (rms) was also explored, as shown in Fig. 6. Charging time varies from 5 min to 30 min at 150 °C. The brightness and driving voltage of the devices are listed in Table 2. Results showed that the brightness increased from 11.9% to 47.6% when charging time increased from 5 min to 30 min, compared with that of the uncharged sample. At a fixed brightness of 269 cd/m$^2$, the driving voltage decreased from 7.6% to 20.46%. The optimal charging time is 30 min in this study. A further increase in charging time would deteriorate the device performance because of surface damage to the electret caused by strong corona plasma.

Fig. 7 displays the luminance images of the uncharged and charged EFBI-PDEL device. The driving voltage is at ac 300 V (rms) and the charging temperature and time are 150 °C and 30 min, respectively. The brightness increased from 269 to 397 cd/m$^2$ when a built-in electric field was introduced in the PDEL device. Results show that the EFBI technique effectively enhanced the luminance of PDEL devices. The improved brightness in the charged device is caused by the built-in electric field further accelerating electrons in the conduction band of the phosphor layer and increasing the electron energy, thus causing more impact excitation with luminescent centers of the phosphor at a lower bias voltage.

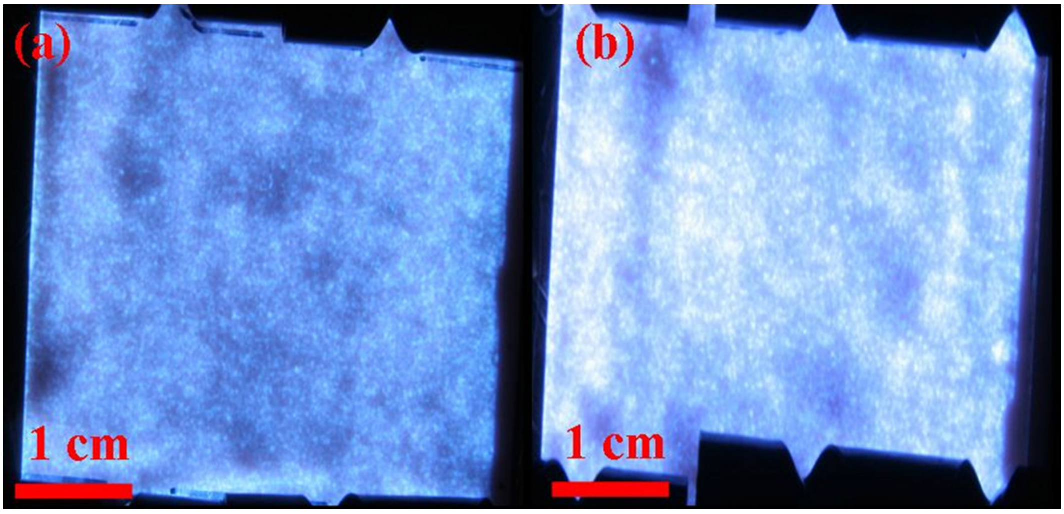


Fig. 7. Luminance images of the (a) uncharged and (b) 150 °C-charged PDEL devices.

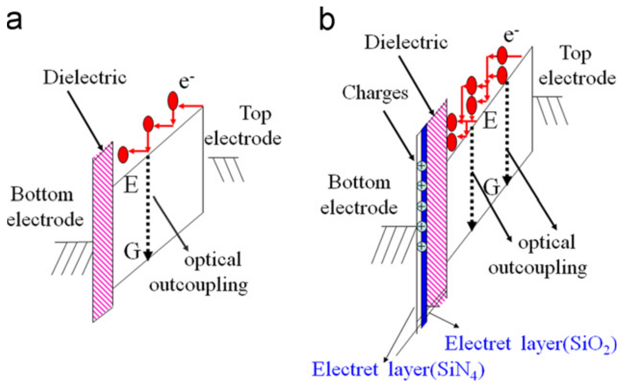


Fig. 8. Energy band diagrams of (a) the traditional PDEL device and (b) the EFBI-PDEL device.

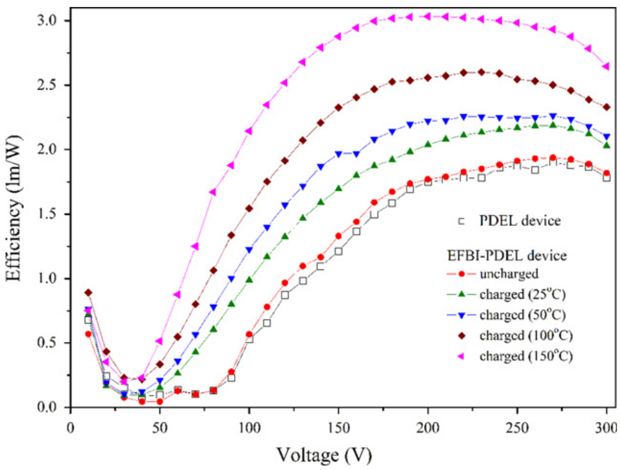


Fig. 9. Efficiency of the EFBI-PDEL device as a function of driving voltage with different charging temperatures.

To understand the mechanism of the enhanced efficiency for the EFBI-PDEL devices, Fig. 8(a) and (b) shows the energy band diagrams of the traditional PDEL and EFBI-PDEL devices, respectively, biased by a positive voltage. The electric field in the traditional PDEL device completely results from the external voltage source applied between the top and bottom electrodes. For the EFBI-PDEL device, the charged electret might store positive

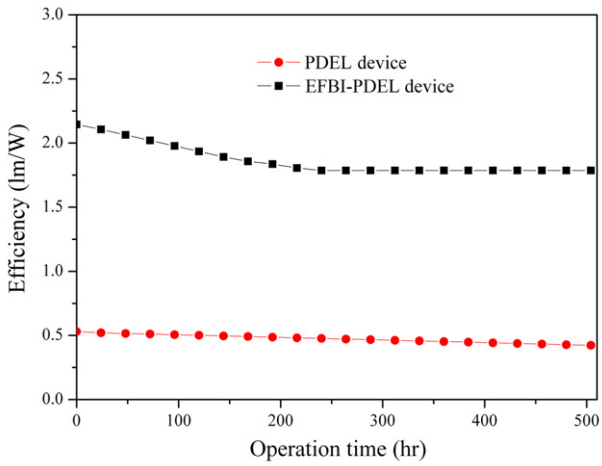


Fig. 10. Efficiency stability of the PDEL devices under ac 100 V.

charges, and thus, increase the electrical field in the device. This results in an increase in the slope of the energy band in the phosphor layer, and hence, raises the electron energy to cause more impact excitation with luminescent centers at lower bias voltages, as shown in Fig. 8(b). For the negative bias, the charges in the electret might reduce the barrier potential of electron injection into the phosphor layer and increase the collision between the luminescent centers and electrons, thus enhancing the luminance of the device [16].

Fig. 9 shows the efficiency of the traditional PDEL device and the proposed EFBI-PDEL devices as a function of driving voltage with different charging temperatures. The efficiency is calculated by the following equation [17]:

$$\eta = \frac{\pi \times L}{I \times V}, \quad (2)$$

where $L$ is the measured luminescence, $I$ is the measured current, and $V$ is the applied voltage. The efficiency of the EFBI-PDEL devices was found to increase with increasing charging temperature. The efficiency of the 150 °C-charged EFBI-PDEL device significantly increased by 45.5% (or 0.827 lm/W) at a driving voltage of 300 V, compared with the uncharged device. Fig. 10 shows the efficiency stability of the PDEL devices under ac 100 V. After a 500-h test, the EFBI-PDEL device still has a higher efficiency than the traditional PDEL one. Particularly, the efficiency of the EFBI-PDEL device almost did not change from 250 to 500 h. This result reveals that the developed EFBI-PDEL device may be applied over the long term.

## 4. Conclusion

This study developed a novel EFBI-PDEL device by using a corona charging system to charge an electret at different temperatures. The existing built-in electric field in the electret lowered the driving voltage of the IEL device, and thus, increased its luminance. At the brightness of 269 cd/m$^2$, the driving voltage of the EFBI-PDEL device charged at 150 °C decreased by 61.4 V (or 20.5%), and when under the ac voltage of 300 V, the brightness of the EFBI-PDEL device increased by 128 cd/m$^2$ (or 47%), compared with the uncharged device. The decreased driving voltage and enhanced brightness resulted because the built-in electric field raises the electron energy in the conduction band of the phosphor layer, and thus, more electron impact ionization occurs to enhance luminance. The proposed EFBI-PDEL device possesses good stability and has potential applications in the backlights of LCD and flat-panel displays in the future.

## Acknowledgments

The authors acknowledge financial support from NSC 101–2221-E-005–065 and Industrial Technology Research Institute, Taiwan, ROC.

## References

[1] J.S. Kim, S.G. Lee, H.L. Park, J.Y. Park, S.D. Han, Mater. Lett. 58 (2004) 1354.
[2] S.D. Han, I. Singh, D. Singh, Y.H. Lee, G. Sharma, C.H. Han, J. Lumin. 115 (2005) 97.
[3] J.H. Park, S.H. Lee, J.S. Kim, A.K. Kwon, H.L. Park, SD. Han, J. Lumin. 126 (2007) 566.
[4] Jin-Young Kim, Taewon Jeong, Shang Hyeun Park, Min Jong Bae, Sunjin Song, Jeonghee Lee, Intaek Han, Donggeun Jung, Chunli Liu, SeGi Yu, Jpn. J. Appl. Phys. 50 (2011) 06GF06.
[5] M.J. Bae, S.H. Park, T.W. Jeong, J.H. Lee, I.T. Han, Y.W. Jin, J.M. Kim, J.Y. Kim, J.B. Yoo, S.G. Yu, Appl. Phys. Lett. 95 (2009) 071901.
[6] K.F. Chen, F.H. Wang, Y.H. Chien, C.C. Chang, M.Y. Chuang, IEEE Electr. Device Lett 32 (2011) 662.
[7] G.M. Sessler, IEEE Trans. Electron Insul 24 (1989) 395.
[8] Z. Xia, R. Gerhard-Multhaupt, W. Kunstler, A. Wedel, R. Danz, J. Phys. D: Appl. Phys 32 (1999) L83–L85.
[9] S. Jeon, C. Kim, Electrochem. Solid-State Lett 9 (2006) G265.
[10] C.J. Huang, Electrochem. Solid-State Lett 4 (2001) F21.
[11] Makoto Honzumi, Kei Hagiwara, Yoshinori Iguchi, Yuji Suzuki, Appl. Phys. Lett. 98 (2011) 052901.
[12] C.L. Cheng, H.Y. Tsai, Electrochem. Solid-State Lett 14 (2011) H21.
[13] X. Zhang, G.M. Sessler, Appl. Phys. Lett. 78 (2001) 2757.
[14] M. Scharnberg, V. Zaporojtchenko, R. Adelung, F. Faupel, C. Pannemann, T. Diekmann, U. Hilleringmann, Appl. Phys. Lett. 90 (2007) 13501.
[15] P.D. Rack, P.H. Holloway, Mater. Sci. Eng R21 (1998) 171.
[16] B.A. Cleary, P.D. Keir, J.C. Hitt, T.K. Plant, J.F. Wager, S.S. Sun, J. SID, Supplement 1 (2000) 51.
[17] J.Y. Kim, S.H. Park, T. Jeong, M.J. Bae, S. Song, J. Lee, I.T. Han, D. Jung, S. Yu, IEEE Tran. Electron. Dev 57 (2010) 1470.